



Numerical Analysis

Numerical simulation of a lid-driven cavity viscoelastic flow at high Weissenberg numbers

Tsorng-Whay Pan, Jian Hao

University of Houston, Department of Mathematics, Houston, TX 77204-3476, USA

Received 21 November 2006; accepted 12 December 2006

Available online 25 January 2007

Presented by Roland Glowinski

Abstract

In this Note we present a finite element method for simulating the Stokes flow of an Oldroyd-B fluid in a lid-driven cavity, which is a stringent test problem at high Weissenberg numbers. The key considerations are: (i) the preservation of the positive definiteness of the conformation tensor at the discrete level; (ii) the use of a coarser mesh when discretizing the conformation tensor to lower the number of high frequency modes; and (iii) additional diffusion to smooth the high frequency modes. The methodologies with the above three features are found to be stable at high Weissenberg numbers. *To cite this article: T.-W. Pan, J. Hao, C. R. Acad. Sci. Paris, Ser. I 344 (2007).*

© 2007 Académie des sciences. Published by Elsevier Masson SAS. All rights reserved.

Résumé

Simulation numérique d'un écoulement viscoélastique dans une cavité entraînée pour des nombres de Weissenberg élevés. Dans cette Note nous présentons une méthode d'éléments finis pour la simulation de l'écoulement d'un fluide viscoélastique de type Oldroyd-B dans une cavité entraînée par une vitesse imposée sur l'une de ses parois. Ce problème est un test modèle pour des nombres de Weissenberg élevés. Les caractéristiques principales de notre méthode sont : (i) la conservation du caractère défini positif du tenseur de conformation au niveau discret ; (ii) l'utilisation d'une maille grossière pour la discrétisation du tenseur de conformation afin de réduire le nombre de modes à haute fréquence ; et (iii) l'introduction d'une diffusion additionnelle pour lisser les modes à haute fréquence. La prise en compte de ces trois mécanismes permet d'obtenir des méthodes stables pour des nombres de Weissenberg élevés. *Pour citer cet article : T.-W. Pan, J. Hao, C. R. Acad. Sci. Paris, Ser. I 344 (2007).*

© 2007 Académie des sciences. Published by Elsevier Masson SAS. All rights reserved.

1. Introduction

Generally, viscoelastic computations in complex flows at high Weissenberg numbers have proven to be a tremendous challenge, in particular for systems where singularities are present. Examples include cavity flows with a steadily moving lid, and only a limited number of computational methods provide satisfactory results [1]. There have been few numerical studies of cavity flows of viscoelastic fluids. There are three important considerations when trying to simulate the time-dependent viscoelastic flows at high Weissenberg numbers. First, the positive definiteness of the

E-mail addresses: pan@math.uh.edu (T.-W. Pan), jianh@math.uh.edu (J. Hao).

conformation tensor has to be preserved at *discrete level* during the *entire time integration*. Fattal and Kupferman [2] reformulated the constitutive equation as equations for the matrix logarithm of the conformation tensor to preserve the positive definiteness. Lozinski and Owen [4] factorized the conformation tensor to get $\boldsymbol{\sigma} = AA^T$ and wrote down the equations for A approximately on the discrete level. Hence the positive definiteness is preserved. Second, the constitutive equation is a hyperbolic equation and lacks diffusion term. In [7], an additional diffusion term added to the constitutive equation for the Oldroyd-B fluid did stabilize the computations. The SUPG methods have also been used widely with finite element methods (see [1]) to stabilize the numerical scheme for solving the constitutive equation. The min-mod limiter used in [2] is known to be very stable, but introduces additional diffusion; indeed the additional diffusion does smooth out some of the high frequency modes and then stabilize the numerical scheme to some extent when solving the constitutive equation. Third, to reduce the number of high frequency modes, we have chosen the finite element for discretizing the conformation tensor defined on a coarser mesh (compared to the mesh for the velocity field); actually in, e.g., [2,6], the discrete conformation tensor were defined on coarser meshes. The methodology, presented in this Note, with the above three features, is found to be stable when simulating lid-driven cavity Stokes flow at high Weissenberg numbers.

2. Formulation of the problem

Let $\Omega = (0, 1) \times (0, 1)$ be the domain occupied by the fluid, Γ the boundary of Ω and $T > 0$. A lid-driven cavity Stokes flow problem of an Oldroyd-B fluid is governed by

$$-\nabla p + \nu_s \Delta \mathbf{u} + \frac{\nu_p}{\lambda_1} \nabla \cdot \boldsymbol{\sigma} = \mathbf{0} \quad \text{in } \Omega \times (0, T), \quad (1)$$

$$\nabla \cdot \mathbf{u} = 0 \quad \text{in } \Omega \times (0, T), \quad (2)$$

$$\frac{\partial \boldsymbol{\sigma}}{\partial t} + (\mathbf{u} \cdot \nabla) \boldsymbol{\sigma} - (\nabla \mathbf{u}) \boldsymbol{\sigma} - \boldsymbol{\sigma} (\nabla \mathbf{u})^T = \frac{1}{\lambda_1} (\mathbf{I} - \boldsymbol{\sigma}) \quad \text{in } \Omega \times (0, T), \quad \boldsymbol{\sigma}(0) = \boldsymbol{\sigma}_0 \quad \text{in } \Omega. \quad (3)$$

Here \mathbf{u} and p are the flow velocity and pressure, $\boldsymbol{\sigma}$ is the conformation tensor, ν_s and ν_p are the solvent and polymer viscosities, λ_1 is a characteristic relaxation time for the fluid, while \mathbf{n} is the unit outward normal vector at the boundary Γ . We also use, if necessary, the notation $v(t)$ for the function $\mathbf{x} \rightarrow v(\mathbf{x}, t)$. To compare numerical results with those in [2], we have chosen the same regularized boundary condition, $\mathbf{g}(\mathbf{x}, t) = (8(1 + \tanh 8(t - 0.5))x^2(1 - x)^2, 0)^T$, on the top boundary, $\{\mathbf{x} \mid \mathbf{x} = (x, 1)^T, 0 < x < 1\}$, and $\mathbf{g}(\mathbf{x}, t) = \mathbf{0}$ on the rest of Γ . The discontinuity of the velocity field at two upper corners has been removed, but the singularity of the conformation tensor at the downstream upper corner at high Weissenberg numbers is still there. There is no inflow boundary condition for the conformation tensor. The Weissenberg number is $We = \lambda_1$.

3. Scheme and discretizations

For the conformation tensor, we have that $\boldsymbol{\psi} = \log \boldsymbol{\sigma}$. (Recall that a symmetric positive definite matrix A can always be diagonalized, $A = R \Lambda R^T$, and that $\log A = R \log \Lambda R^T$.) In [2], with \mathbf{u}^n being a divergence-free velocity field and $\boldsymbol{\sigma}$ a symmetric positive definite tensor field, the velocity gradient $\nabla \mathbf{u}^n$ can be decomposed as $\nabla \mathbf{u}^n = \boldsymbol{\omega}_n + B_n + N_n \boldsymbol{\sigma}^{-1}$ where $\boldsymbol{\omega}_n$ and N_n are anti-symmetric, and B_n is symmetric, traceless, and commutes with $\boldsymbol{\sigma}$. Combining the Lie's scheme [3] and the matrix logarithm of the conformation tensor yields the scheme as follows:

For $n \geq 0$, $\boldsymbol{\sigma}^n$ (and $\boldsymbol{\psi}^n$) being known, we solve \mathbf{u}^{n+1} and p^{n+1} via the solution of the problem:

$$-\nabla p^{n+1} + \nu_s \Delta \mathbf{u}^{n+1} = -\frac{\nu_p}{\lambda_1} \nabla \cdot \boldsymbol{\sigma}^n \quad \text{in } \Omega, \quad (4)$$

$$\nabla \cdot \mathbf{u}^{n+1} = 0 \quad \text{in } \Omega, \quad (5)$$

$$\mathbf{u}^{n+1} = \mathbf{g}(t^{n+1}) \quad \text{on } \Gamma. \quad (6)$$

Next, we solve $\boldsymbol{\psi}^{n+1}$ via the following steps: first solve

$$\frac{\partial \boldsymbol{\psi}}{\partial t} + (\mathbf{u}^{n+1} \cdot \nabla) \boldsymbol{\psi} = \mathbf{0} \quad \text{in } \Omega \times (t^n, t^{n+1}), \quad \boldsymbol{\psi}(t^n) = \boldsymbol{\psi}^n \quad \text{in } \Omega, \quad (7)$$

and set $\boldsymbol{\psi}^{n+1/2} = \boldsymbol{\psi}(t^{n+1})$. Then solve

$$\frac{\partial \boldsymbol{\psi}}{\partial t} - [\boldsymbol{\omega}_{n+1} \boldsymbol{\psi} - \boldsymbol{\psi} \boldsymbol{\omega}_{n+1}] - 2B_{n+1} = \frac{1}{\lambda_1} (\mathbf{e}^{-\boldsymbol{\psi}} - \mathbf{I}) \quad \text{in } \Omega \times (t^n, t^{n+1}), \quad \boldsymbol{\psi}(t^n) = \boldsymbol{\psi}^{n+1/2} \quad \text{in } \Omega, \quad (8)$$

and set $\boldsymbol{\psi}^{n+1} = \boldsymbol{\psi}(t^{n+1})$ and $\boldsymbol{\sigma}^{n+1} = \mathbf{e}^{\boldsymbol{\psi}^{n+1}}$.

Concerning the *space approximation*, we have used P_1 -iso- P_2 and P_1 finite elements for the velocity field and pressure, respectively, and P_1 finite element defined on the pressure mesh for each component of the log-conformation tensor. The Stokes problem (4)–(6) is solved by an Uzawa/conjugate gradient algorithm [3]. The advection problem (7) is solved by a wave-like equation method (e.g., see [3]) with first order upwind treatment for the advection, $\mathbf{V} \cdot \nabla f$, at each sub-timestep. In (8) $\boldsymbol{\omega}_{n+1}$ and B_{n+1} are obtained from $\nabla \mathbf{u}^{n+1}$, which is computed via an L^2 -projection on the pressure mesh. Then problem (8) is solved at each mesh point by a 2nd order Runge–Kutta method since the trapezoidal quadrature rule is used for numerical integration.

4. Numerical experiments

We have considered the numerical simulation of a lid-driven cavity Stokes flow for an Oldroyd-B fluid. The initial condition for $\boldsymbol{\sigma}$ is $\boldsymbol{\sigma}_0 = \mathbf{I}$. The viscosities, ν_s and ν_p , in all calculations are equal to 1. The relaxation time λ_1 is 1 or 3 ($We = 1$ or 3, respectively). The meshes \mathcal{T}_h and \mathcal{T}_{2h} are uniform triangular meshes. For the case of $We = 1$, results obtained with $h = 1/128$ and $1/256$ are computed with timestep $\Delta t = 0.001$. The history of the kinetic energy and the streamlines are shown in Fig. 1 for $h = 1/256$. The center of the core vortex region shifts in the upstream direction as observed in the experiments [5]. The cross sections of the velocity field and the log-conformation tensor are shown in

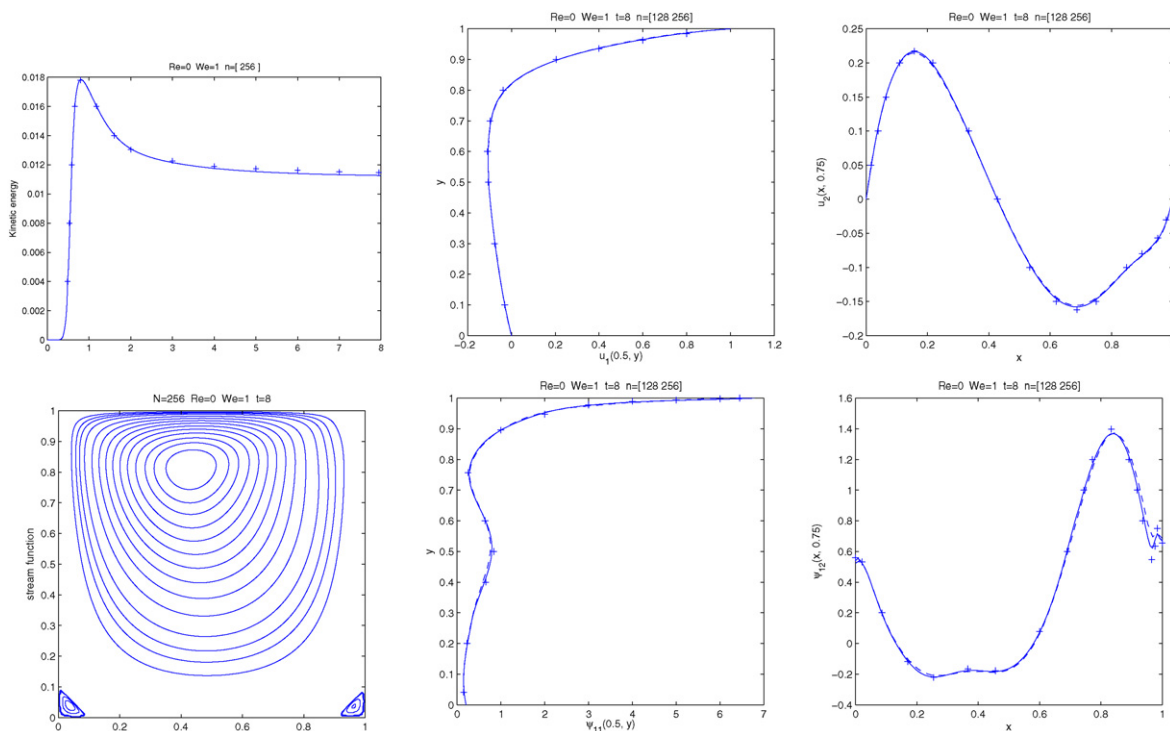


Fig. 1. (a) The history of the kinetic energy, $\frac{1}{2} \|\mathbf{u}_h\|_2^2$ (upper left) and the streamlines (lower left) for $h = 1/256$. (b) The cross-sections: $u_1(0.5, y)$ (upper middle), $u_2(x, 0.75)$ (upper right), $\psi_{11}(0.5, y)$ (lower middle), and $\psi_{12}(x, 0.75)$ (lower right) for $h = 1/128$ (dashed line) and $1/256$ (solid line) at $t = 8$ for $We = 1$. The marks of ‘+’ are results obtained in [2].

Fig. 1. (a) L'évaluation de l'énergie cinétique, $\frac{1}{2} \|\mathbf{u}_h\|_2^2$ (gauche supérieure) et les lignes de courant (gauche inférieure) pour $h = 1/256$. (b) Les sections transverses : $u_1(0, 5, y)$ (milieu supérieure), $u_2(x, 0, 75)$ (droite supérieure), $\psi_{11}(0, 5, y)$ (milieu inférieure), et $\psi_{12}(x, 0, 75)$ (droite inférieure) pour $h = 1/128$ (ligne traitillée) et $1/256$ (ligne solide) à $t = 8$ pour $We = 1$. Les symboles « + » correspondent aux résultats obtenus dans [2].

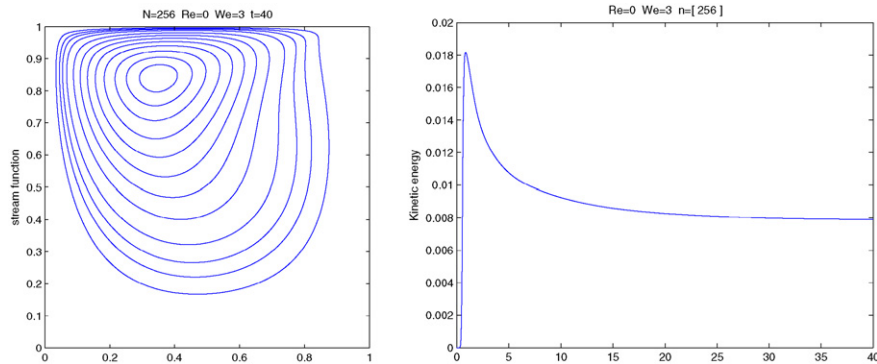


Fig. 2. The streamlines (left) and the history of the kinetic energy (right) for $We = 3$.

Fig. 2. Les lignes de courant (gauche) et l'évaluation de l'énergie cinétique (droite) pour $We = 3$.

Fig. 1. They are all in good agreement with the results shown in [2]. For the case of $We = 3$, the history of the kinetic energy and the streamlines in Fig. 2, for $h = 1/256$ and $\Delta t = 0.001$, show that the method is stable, which was not obtained in [2].

Acknowledgements

We acknowledge the helpful comments of R. Glowinski, D.D. Joseph, A. Lozinski, A. Caboussat, P. Singh and the support by NSF (grants DMS-0209066, DMS-0443826).

References

- [1] F.P.T. Baaijens, Mixed finite element methods for viscoelastic flow analysis: a review, *J. Non-Newtonian Mech.* 79 (1998) 361–385.
- [2] R. Fattal, R. Kupferman, Time-dependent simulation of viscoelastic flows at high Weissenberg number using the log-conformation representation, *J. Non-Newtonian Fluid Mech.* 126 (2005) 23–37.
- [3] R. Glowinski, Finite element methods for incompressible viscous flow, in: P.G. Ciarlet, J.L. Lions (Eds.), *Handbook of Numerical Analysis*, vol. IX, North-Holland, Amsterdam, 2003.
- [4] A. Lozinski, R.G. Owen, An energy estimate for the Oldroyd-B model: theory and applications, *J. Non-Newtonian Fluid Mech.* 112 (2003) 161–176.
- [5] P. Pakdel, S.H. Spiegelberg, G.H. McKinley, Cavity flows of elastic liquids: two-dimensional flows, *Phys. Fluids* 9 (1997) 3123–3140.
- [6] P. Saramito, Efficient simulation of nonlinear viscoelastic fluid flows, *J. Non-Newtonian Fluid Mech.* 60 (1995) 199–223.
- [7] R. Sureshkumar, A.N. Beris, Effect of artificial stress diffusivity on the stability of numerical calculations and the flow dynamics of time-dependent viscoelastic flows, *J. Non-Newtonian Fluid Mech.* 60 (1995) 53–80.